Review

Effect of Spring-Mass-Damper Pedestrian Models on the Performance of Low-Frequency or Lightweight Glazed Floors

Chiara Bedon [1,*] **and Filipe A. Santos** [2]

1   Department of Engineering and Architecture, University of Trieste, 34127 Trieste, Italy
2   CERIS-NOVA, Department of Civil Engineering, NOVA School of Science and Technology, Universidade NOVA de Lisboa, 2829-516 Caparica, Portugal; fpas@fct.unl.pt
*   Correspondence: chiara.bedon@dia.units.it; Tel.: +39-04-0558-3837

Abstract: For structural design purposes, human-induced loads on pedestrian systems can be described by several simplified (i.e., deterministic equivalent-force models) or more complex computational approaches. Among others, the Spring-Mass-Damper (SMD), Single Degree of Freedom (SDOF) model has been elaborated by several researchers to describe single pedestrians (or groups) in the form of equivalent body mass m, spring stiffness k and damping coefficient c. For all these literature SMD formulations, it is proved that the biodynamic features of walking pedestrians can be realistically reproduced, with high computational efficiency for vibration serviceability assessment of those pedestrian systems mostly sensitive to human-induced loads (i.e., with vibration frequency $f_1 < 8$ Hz). Besides, the same SMD proposals are characterized by mostly different theoretical and experimental assumptions for calibration. On the practical side, strongly different SMD input parameters can thus be obtained for a given pedestrian. This paper focuses on a selection of literature on SMD models, especially on their dynamic effects on different structural floor systems. Four different floors are explored (F#1 and F#2 made of concrete, F#3 and F#4 of glass), with high- or low-frequency, and/or high- (>1/130th) or low- (1/4th) mass ratio, compared to the occupant. Normal walking scenarios with frequency in the range $f_p = 1.5–2$ Hz are taken into account for a total of 100 dynamic simulations. The quantitative comparison of typical structural performance indicators for vibration serviceability assessment (i.e., acceleration peak, RMS, CREST) shows significant sensitivity to input SMD assumptions. Most importantly, the sensitivity of structural behaviours is observed for low-frequency systems, as expected, but also for low-mass structures, which (as in the case of glazed floor solutions) can be characterized by the use of lightweight modular units with relatively high vibration frequency. As such, major attention can be required for their vibrational analysis and assessment.

Keywords: human-induced effects; pedestrian structures; Spring-Mass-Damper (SMD) models; Single Degree of Freedom (SDOF) model; numerical analysis; structural performance indicators

1. Introduction

For structures in general, but especially for structural systems characterized by low vibration frequency and high slenderness like bridges or some types of floors, the analysis of Human-Structure Interaction (HSI) phenomena and the quantification of their effects on structures is of crucial importance for vibration serviceability assessment [1,2], and generally requires dedicated calculations [3]. So far, many literature efforts have been thus elaborated in decades to facilitate the mathematical description and analysis of typical boundaries and loading conditions of technical interest [2].

Among others [3], biodynamic schemes of single (or group) pedestrians can be efficiently represented by Spring-Mass-Damper (SMD) and Single Degree of Freedom (SDOF) models able to capture the motion features and effects of occupants (Figure 1). In this regard, a multitude of sound and robust analytical proposals can be found in the literature, with experimental and numerical validation of basic assumptions for SMD calibration, see

for example [4–8] and others. Furthermore, SMD models are especially recommended for structural systems with low frequency (i.e., $f_1 < 8$ Hz [2]) and thus higher vulnerability to vibrations induced by pedestrians [1,2]. Also, SMD models can efficiently include the effects of pedestrians in the lateral direction [9].
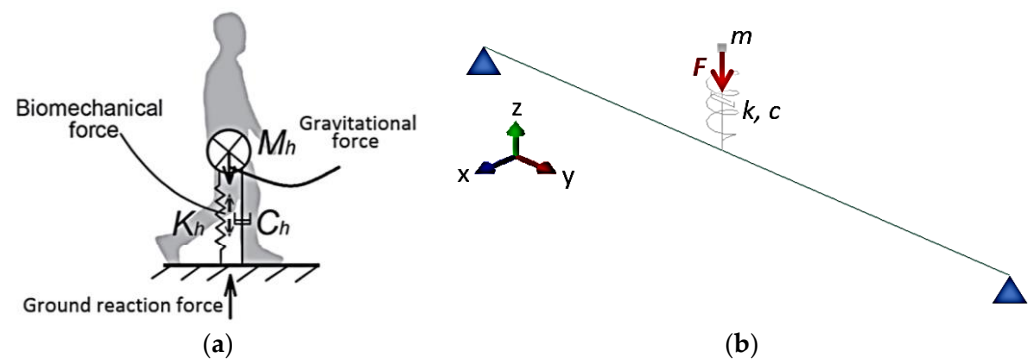
Figure 1. Biodynamic pedestrian model: (**a**) schematic representation of Spring-Mass-Damper (SMD), Single Degree of Freedom (SDOF) model (figure reprinted from [8] with permission from Elsevier©, copyright license number agreement 5458701302374, December 2022) and (**b**) example of presently developed numerical model for Human-Structure Interaction (HSI) analysis.

SMD models are, in fact, particularly advantageous because they can provide major detailing compared to deterministic loading strategies like in [2,3]. From a practical point of view, SMD approaches are still computationally efficient and thus represent a practical tool for vibration serviceability studies. The simplest calculation approach is represented by the use of equivalent time-varying forces able to simulate the ground-reaction force due to pedestrians. While of simple application, these equivalent-force deterministic procedures have a major limitation in the description of reaction forces by the Fourier series. Such an assumption is particularly efficient for computational purposes but disregards the interaction of pedestrians with structures, namely HSI phenomena. As such, equivalent force methods are accurate for specific structural configurations, especially for systems in which the dynamic interaction with pedestrians' motion is irrelevant.

In structural terms, the intrinsic advantage of SMD biodynamic pedestrian models are to describe pedestrians in terms of equivalent mass m (which is lumped in the body Centre-of-Mass (CoM)), stiffness k and damping coefficient c terms, which are expected to interact with the structure during motion of occupants. Overall, the dynamic problem is represented by a moving SMD biodynamic pedestrian model (with frequency f_m), which interacts with a substructure characterized by mass M_s, fundamental vibration frequency f_1, damping ratio ζ_s, and thus possible sensitivity to vibration issues (Figure 1b). Even more complex, bipedal, and three-dimensional biodynamic models could also be used for sophisticated HSI calculations, see for example [10–13].

As a common assumption of these literature formulations, low-frequency pedestrian systems (usually represented by laboratory prototypes) or rigid contrast systems are taken into account regardless of other structural parameters of interest, like, for example, the mass of structure M_s in relation to pedestrians (and thus possible additional HSI interaction with occupants). For the SMD models in [5,6], for example, the experimental calibration of input biodynamic parameters was carried out on an 11.63 m long prototype footbridge with $f_1 = 4.27$ Hz and $\xi_s = 1\%$. A prototype of a walkway consisting of a massive steel-concrete composite deck was used for the laboratory investigations reported in [7]. Rigid platforms were also used for the SMD validations reported in [5,7,8].

In this paper, a selection of existing SMD approaches is taken into account for structural performance assessment. The attention is primarily given to glazed floors which are mostly characterized by specific fundamental vibration frequency f_1 and mass M_s parameters, compared to other construction typologies. To facilitate the comparative analysis, four

different SMD proposals from earlier studies (SMD-1 to SMD-4, in the following, see [5–8]) are applied to four different floor configurations (F#1 to F#4, in the following), under normal walking scenarios of a single pedestrian. In doing so, two different glazed floor systems (F#3 and F#4) are analyzed and addressed towards two different concrete configurations (F#1 and F#2). From the total of 100 numerical analyses/configurations, the attention is focused on typical performance indicators of primary interest to characterize and assess the vibration response of structures (like acceleration peak, RMS acceleration and CREST factor).

In terms of F#1 to F#4 floor systems, most importantly, various combinations of vibration frequency f_1 and structural mass M_s are taken into account. For the concrete floors (F#1 and F#2), for example, the M_s term is generally high compared to pedestrians, regardless of the vibration frequency f_1 (i.e., > or <8 Hz). In the case of structural glass systems like F#3 and F#4 solutions [14,15], on the other side, basic structural components are typically characterized by structural mass M_s which can often be relatively low compared to occupants, and by vibration frequency f_1 which is not necessarily "low" [16–18], see Figure 2. Dedicated studies are thus recommended to address HSI phenomena on glazed floors, especially under unfavourable operational and ambient conditions (see for example [19,20]).

(**a**)

(**b**)
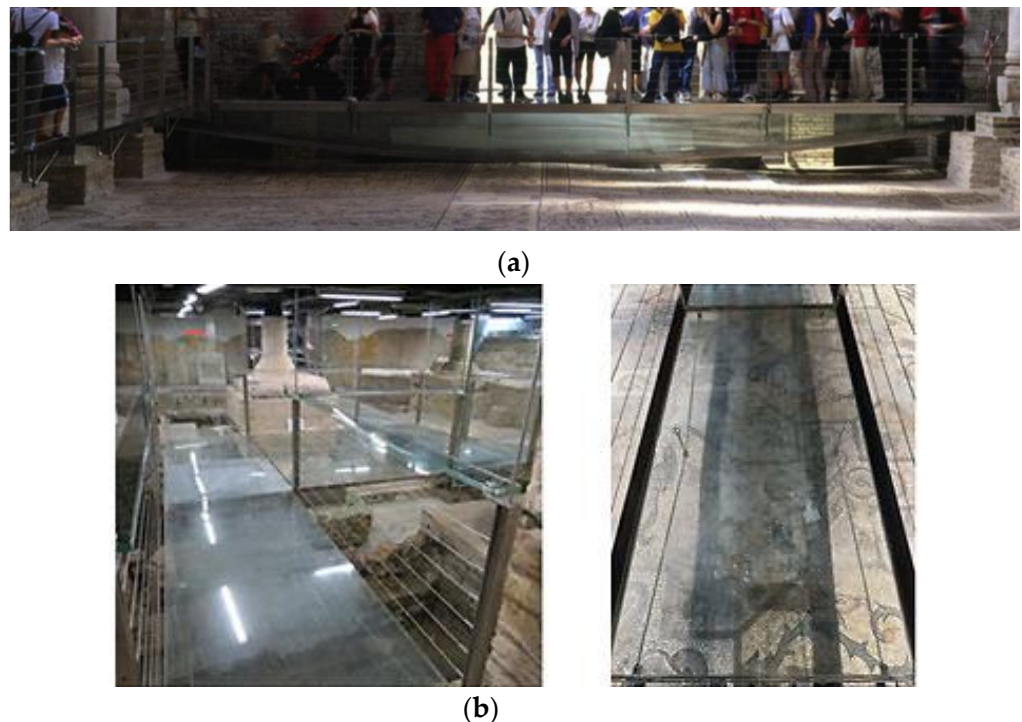
Figure 2. Examples of glass pedestrian systems ((**a**) reproduced from [16] with permission from Elsevier©, copyright license number agreement 5502960982555, March 2023; (**b**) reproduced from [18] under the terms and conditions of a CC-BY copyright license agreement).

In general terms, regardless of the structural floor typology, the analysis of input SMD parameters show, at first, that major modifications can be found in terms of pedestrian characterization, even under similar walking conditions and sub-structure dynamic parameters. As such, relevant effects can be expected about the performance indicators of primary interest for structural analysis and vibration serviceability assessment. This aspect reflects on the design and verification tasks and decisions of the final user/designer and thus necessitates robust validation, especially for innovative structural typologies.

A more detailed comparative analysis of quantitative response indicators for the examined floor systems, moreover, allows defining of additional correlations for the observed responses as a function of floor features. As shown, the collected numerical results from

selected SMD models are mostly aligned for high-frequency and high-mass floors (like F#1 concrete systems in the present study). On the other side, major sensitivity of estimated structural performance indicators is found for F#2 concrete system (and this is in line with expectations due to its low frequency), but also for the F#3 and F#4 glazed systems, thus suggesting specific studies for this structural typology.

2. Research Methods, Materials and Models

The presently reported numerical investigation was carried out in ABAQUS [21]. A set of walking configurations was examined under the effects of a single pedestrian (M = 80 kg) moving on the four slab systems in Section 2.1.

The parametric investigation was performed by considering the four different SMD models in Section 2.2 for the same pedestrian moving on each floor, while the walking frequency was modified in the range f_p = 1.5–2 Hz (0.1 Hz the increment) for a total of 100 dynamic simulations.

2.1. Selected Floor Systems

To address the effects of various SMD formulations, attention was first given to a selection of concrete slabs (F#1 and F#2 in Table 1), characterized by high or low vibration frequency f_1, respectively, with high structural mass M_s compared to the occupant. Therefore, two additional low-frequency and low-mass floor systems (F#3 and F#4 in Table 1), inspired by earlier literature studies reported in [16–18] and Figure 2, were also considered in the present analysis. More in detail, the F#3 system coincides with the suspension platform in Figure 2a, while F#4 represents the modular system in Figure 2b. As shown in Table 1, the primary feature of the F#3 system is the low vibration frequency (f_1 < 8 Hz) but still relatively high mass Ms, compared to pedestrians (1/134th). This is not the case of the F#4 system, in which the slab is again composed of structural glass, and M_s is relatively small compared to pedestrians (1/4th), whilst the fundamental vibration frequency f_1 is relatively high for vibrational assessment purposes.

Table 1. Summary of basic features for the examined floor configurations (with M = 80 kg).

| Floor	Material	Span [m]	Surface [m²]	Frequency f_1 [Hz]	Mass M_s [kg]	M/M_s
F#1	Concrete	5	30	11.05	10,350	1/130
F#2	Concrete	5	30	5.30	3530	1/44
F#3	Glass	14.5	40.6	7.28 *	10,730	1/134
F#4	Glass	2.65	3.58	14.30 *	320	1/4

* = experimental data from [16,18].

It would be expected that the concrete F#1 and glass F#4 systems (i.e., f_1 > 8 Hz) can be representative of "rigid" floor systems, which are minimally sensitive to HSI phenomena. Conversely, F#2 and F#3 (with f_1 < 8 Hz) are expected to be the most affected by human-induced loads. Overall, mass contributions in Table 1 are another important parameter to address.

In the parametric numerical analysis, a conventional ξ_s = 3% damping ratio was taken into account for concrete slabs F#1 and F#2 [2]. In the case of the glass floor systems F#3 and F#4, the input damping ratio was set at ξ_s = 2% [19,20].

2.2. Selected SMD Models of Literature

Over the years, several experimental and theoretical studies have been elaborated to efficiently calibrate the input SMD features of a pedestrian on typically slender and flexible structures (Figure 3). The attention of the present investigation, among others, was focused on the effects of SMD proposals described in [5–8].
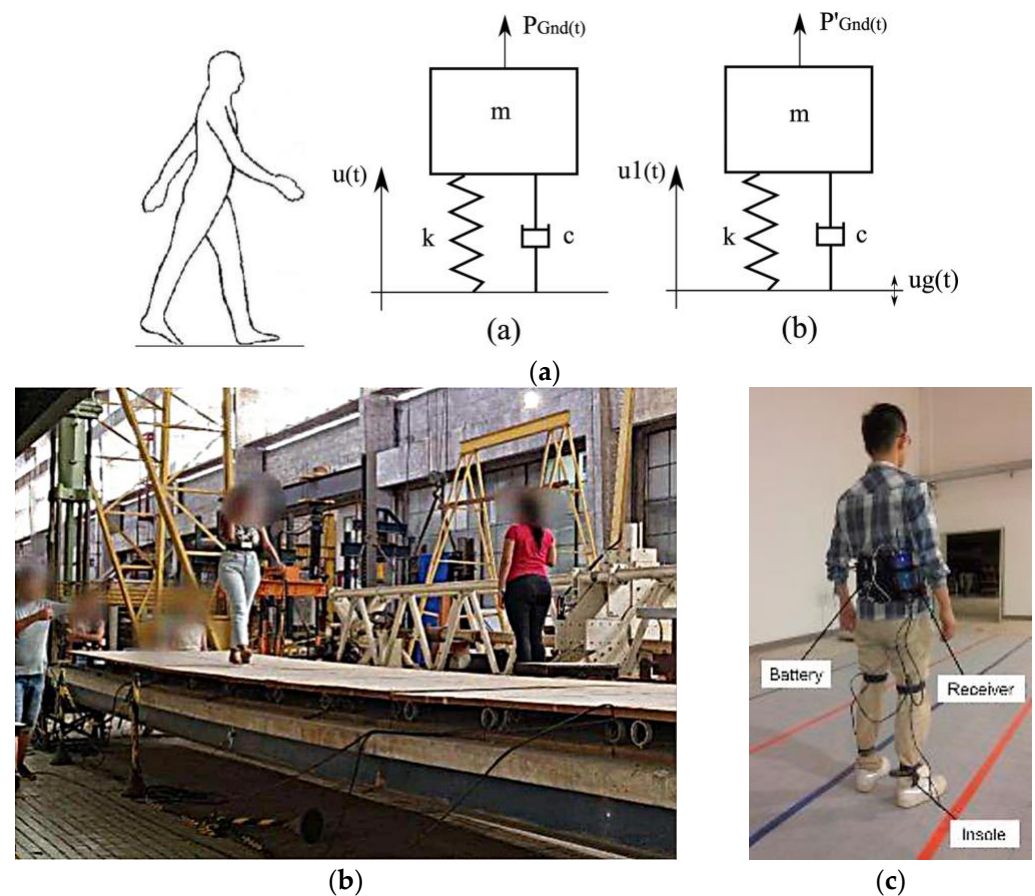
Figure 3. Biodynamic pedestrian models: (**a**) schematic mechanical model of a pedestrian on rigid or flexible structure (figure reproduced from [6] with permission from Elsevier©, copyright license number agreement 5458710774818, December 2022); (**b**) experimental setup for pedestrian walking on flexible laboratory platform (figure reproduced from [7] with permission from Elsevier©, copyright license number agreement 5458711054568, December 2022); (**c**) experimental analysis by Wang et al. to measure the ground reaction force (figure reproduced from [8] with permission from Elsevier©, copyright license number agreement 5458710094483, December 2022).

Silva et al. [5], "SMD-1" in the following, validated their formulation towards experiments carried out on a low-frequency footbridge prototype ($f_1 < 5$ Hz). The authors elaborated a regression model for biodynamic SDOF parameters. The equivalent mass m, the damping coefficient c and the spring stiffness k can be calculated as a function of walking frequency f_p and pedestrian mass M. The term c is fitted to m, and the stiffness term k derives from c, where:

$$m = m(f_p, M) = 97.082 + 0.275M - 37.52f_p \tag{1}$$

$$c = c(m) = 107.455 + 16.208m \tag{2}$$

$$k = k(c) = 5758.441 + 11.103c \tag{3}$$

A similar working assumption for SMD elaboration and validation can be found in the proposal by Toso et al. [6] ("SMD-2" model, in the following). More precisely, their experimental evidence was processed from 35 instrumented individual pedestrians and further elaborated by Artificial Neural Network (ANN) to correlate the biodynamic parameters to basic walking features. A rigid platform ($f_1 = 30.1$ Hz) was initially used in the experiments, and then the SMD characterization was extended to a flexible footbridge prototype as in [5], with $f_1 < 5$ Hz. It was found, for example, that the ANN was able to act

efficiently with minimum uncertainty, and the final SMD proposal resulted in the following pedestrian parameters:

$$m = m(f_p, M) = -231.34 + 3.69M + 154.06f_p - 1.97Mf_p + 0.005M^2 - 15.25f_p^2 \quad (4)$$

$$c = c(M, m) = -1115.69 + 92.56M - 108.94m + 2.91Mm - 1.33M^2 - 1.30m^2 \quad (5)$$

$$k = k(M, f_p) = 75601.45 - 1295.32M - 33786.75f_p + 506.44Mf_p + 3.59M^2 + 539.39f_p^2 \quad (6)$$

The third SMD calibration approach, consisting of the method proposed by Pfeil et al. [7] and noted as the "SMD-3" model in the present study, included several experimental measurements of pedestrians moving on a rigid floor (coinciding with the laboratory foundation slab) and then on a flexible walkway like in Figure 3b, composed of steel-concrete composite deck and characterized on top by two medium-density fiberboard plates, with f_1 = 17 Hz [22]. The monitored experimental configurations included slow, normal, or fast walks.

The SMD-3 formulation from [7] assumes a reduction in equivalent mass m of pedestrian and a spring stiffness k which is linearly proportional to m:

$$m = m(f_p, M) = 0.874M - 9.142f_p + 12.94 \quad (7)$$

$$k = k(m) = 360.3m - 1282.5 \quad (8)$$

In such a formulation, the damping coefficient c must be calculated from iterative calculations in terms of damping ratio ξ, as a function of the damped SDOF frequency f_{md}.

It is, in fact, assumed that:

$$\xi = \xi(f_{md}) = -20.818f_{md} + 87.513 \quad (9)$$

and

$$f_m = \sqrt{\frac{k}{m}} \bullet \frac{1}{2\pi} \quad (10)$$

with

$$f_{md} = f_m \bullet \sqrt{1 - \xi^2} \quad (11)$$

The iterative calculation on Equation (9) must be thus repeated until the damping ratio converges.

Finally, the proposal by Wang et al. [8], herein detected as the "SMD-4" model, assumes that $m = M$ and:

$$f_m = f_m(f_p) = 0.3049f_p + 1.367 \quad (12)$$

$$c = c(f_p) = -0.2116f_p + 0.8737 \quad (13)$$

thus, k comes from Equation (10), where the stiffness k can be extrapolated based on $m = M$ and assuming for f_m the value given by Equation (12) once f_p is assigned.

The so-derived input SMD parameters from the above-summarized pedestrian models are shown in Figure 4, as a function of the assigned walking frequency f_p, with evidence of undamped frequency f_m of the pedestrian model (from Equation (10)), equivalent mass m, spring stiffness k and damping coefficient c respectively. Most importantly, the relatively wide scatter of biodynamic pedestrian features can be seen when SMD-1 to 4 formulations is used—regardless of the type and features of floors—to describe the equivalent walking features of a single pedestrian (M = 80 kg). As such, variations are also expected in terms of corresponding performance indicators.
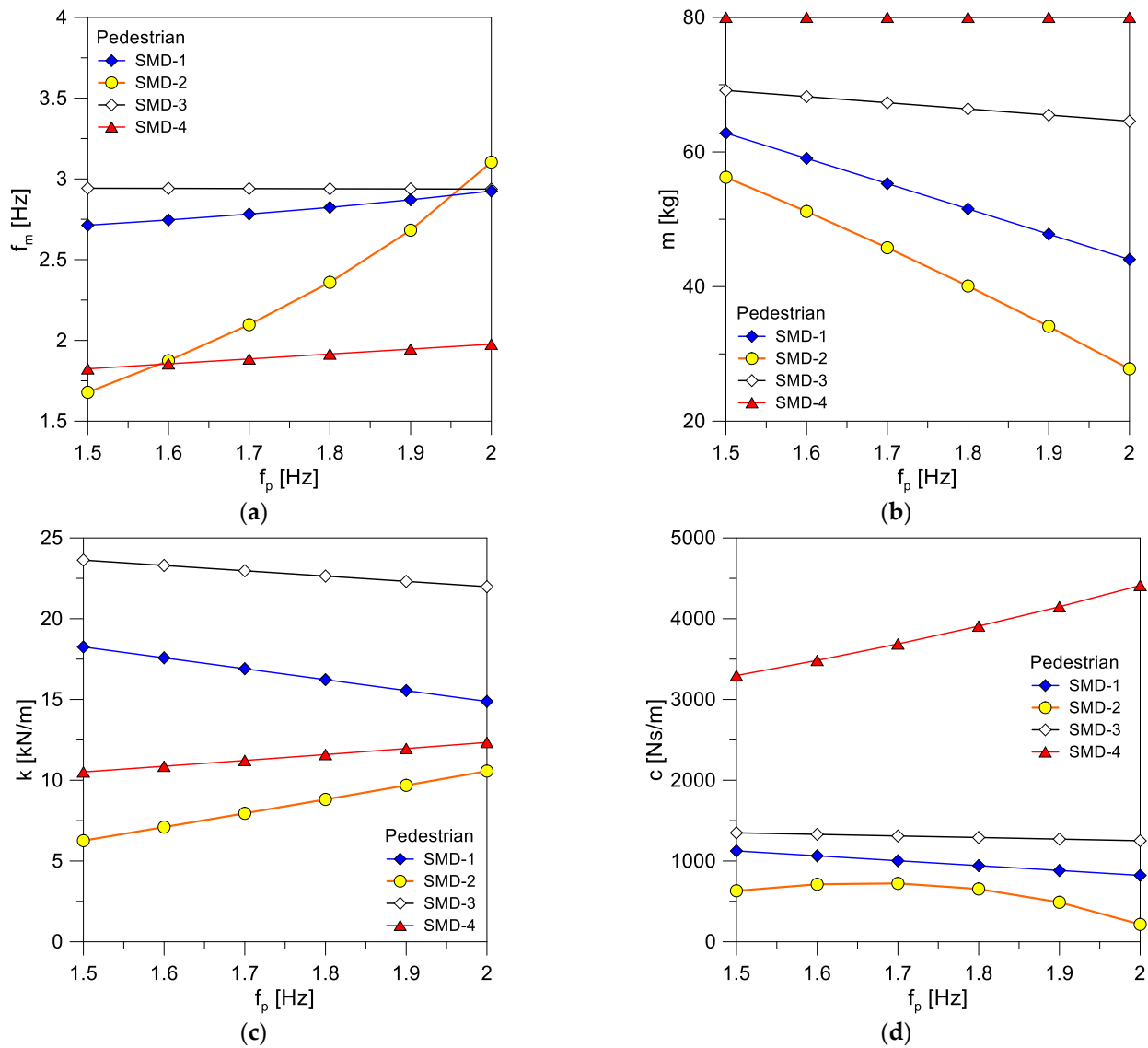
Figure 4. Selected biodynamic pedestrian models (with M = 80 kg) and variation of input SMD parameters with walking frequency f_p: (**a**) pedestrian model frequency f_m, (**b**) equivalent mass m, (**c**) spring stiffness k, (**d**) damping coefficient c.

2.3. Equivalent-Force Deterministic Model

As a reference for modelling, the consolidated analytical proposal in [2] was taken into account to introduce the vertical reaction forces for the present numerical investigation. Following [2], the single footfall is, in fact, assumed to transfer a force time history equal to (in Newton):

$$F(t) = 746 \sum_{i=1}^{8} K_i t^i = 746 \left(K_1 t + K_2 t^2 + K_3 t^3 + K_4 t^4 + K_5 t^5 + K_6 t^6 + K_7 t^7 + K_8 t^8 \right) \quad (14)$$

with K_i the coefficients in Table 2 and t the time (in seconds) within a single footfall, where:

$$t_s = -0.515 f_p^3 + 3.2242 f_p^2 - 6.9773 f_p + 5.8531 \quad (15)$$

denotes the duration of a single footfall (in seconds) of walking frequency f_p (in Hertz), see the example in Figure 5.

Table 2. Definition of input coefficients K_i for Equation (14), based on walking frequency f_p.

Coefficient	f_p (Hz)	
	$\leq$**1.75**	**1.75 $\div$ 2**
K_1	$-8 f_p + 38$	$24 f_p - 18$
K_2	$376 f_p - 844$	$-404 f_p + 521$
K_3	$-2804 f_p + 6025$	$4224 f_p - 6274$
K_4	$6308 f_p - 16{,}573$	$-29{,}144 f_p + 45{,}468$
K_5	$1732 f_p - 13{,}619$	$109{,}976 f_p - 175{,}808$
K_6	$-24{,}638 f_p + 16{,}045$	$-217{,}424 f_p + 353{,}403$
K_7	$31{,}836 f_p - 33{,}614$	$212{,}776 f_p - 350{,}259$
K_8	$-12{,}948 f_p + 15{,}532$	$-81{,}572 f_p + 135{,}624$
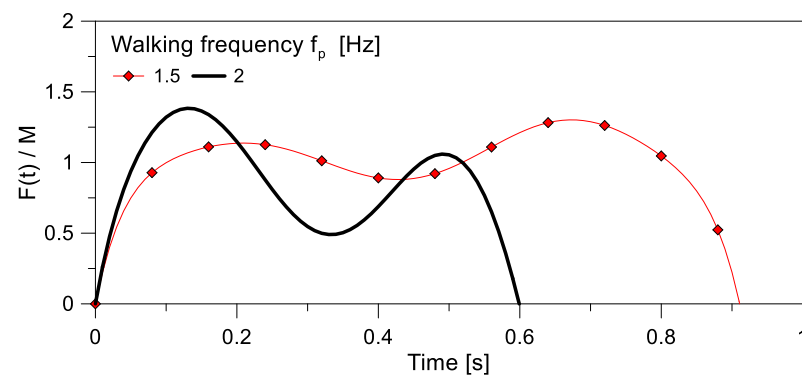
Figure 5. Example of analytical description of single footfall vertical load, based on the equivalent-force deterministic model as in Equation (14). Vertical load F (in Newton) is normalized to the mass of the pedestrian ($M = 80$ kg).

The corresponding walking speed is given by:

$$v_s = 1.67 f_p^2 - 4.83 f_p + 4.5 \tag{16}$$

Input coefficients are listed in Table 2 with specific attention to the range of interest in the present study ($f_p = 1.5 \div 2$ Hz).

3. Parametric Numerical Analysis

3.1. Modelling

The numerical analysis was carried out in ABAQUS/Standard for all the examined configurations in dynamic Implicit simulations. To this aim, the reference model for structural floors and pedestrians was assembled in accordance with Figure 1b, that is, in the form of shell elements for the structure and a coupled SMD model representative of the pedestrian. The lumped mass m was positioned at a given height of 1.1 m from the walking surface, which is in line with the CoM of examined volunteer (based on [16–20]). A spring/dashpot element was also used to introduce the equivalent spring k and damping coefficient c terms.

To this aim, the input SMD parameters for pedestrians were taken from Section 2 and Figure 4 as a function of the imposed f_p. Moreover, comparative calculations were carried out towards the deterministic, equivalent force loading approach as in Equation (14), based on a rigid uncoupled SDOF assumption, with $m = M$ ("RU" model, in the following).

In terms of damping, a conventional Rayleigh approach was taken into account to define the mass-proportional and stiffness-proportional damping ratio terms of each floor configuration [23]. More specifically, they were calculated as:

$$\alpha = \zeta_s \frac{2\omega_1 \omega_2}{\omega_1 + \omega_2} \tag{17}$$

$$\beta = \xi_s \frac{2}{\omega_1 + \omega_2} \tag{18}$$

with ω_1, ω_2 are the natural circular frequencies corresponding to the first and second vibration modes of the F#1-to-#4 floor systems with input features summarized in Table 1.

3.2. Structural Performance Indicators

The comparative analysis was elaborated on the base of acceleration time histories on the examined F#1 to F#4 floors, and a typical example can be seen in Figure 6. In doing so, the control point was detected in the mid-span section of each system. According to several literature documents, the parametric numerical results were addressed in terms of traditional performance indicators for vibration serviceability issues. For the examined range of walking patterns, the acceleration time histories of investigated floor systems were first elaborated to express the Root Mean Squared (RMS) acceleration value, that is:

$$a_{Z,RMS} = \sqrt{\frac{1}{t_n - t_{n-1}} \int_{t_{n-1}}^{t_n} a_Z^2(t) \, dt} \tag{19}$$
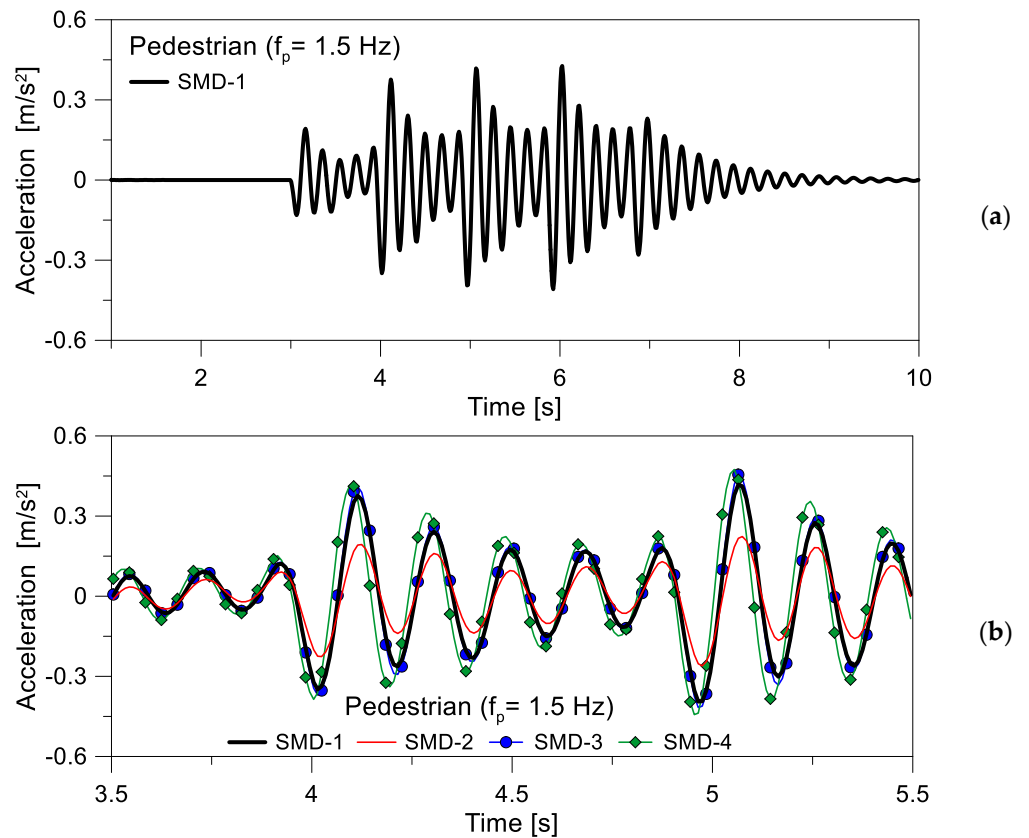
Figure 6. Example of typical dynamic response for the F#2 concrete system under normal walk (M = 80 kg, f_p = 1.5 Hz): (**a**) acceleration time history on the structure and (**b**) comparative detail (ABAQUS).

Additional comparisons were carried out, among the selected loading approaches, in terms of peak acceleration on the floor ($a_{Z,peak}$) and CREST factor for each walking frequency, that is:

$$CREST = \frac{a_{Z,peak}}{a_{Z,RMS}} \tag{20}$$

4. Discussion of Numerical Results

4.1. Floor Response

For the selected walking configurations, especially f_p, typical vibration responses were found highly sensitive to floor system features, both in the presence of low-frequency and low-mass parameters. Typical trends for selected walking frequencies are reported in Figure 7 in terms of RMS acceleration based on the RU modelling strategy.
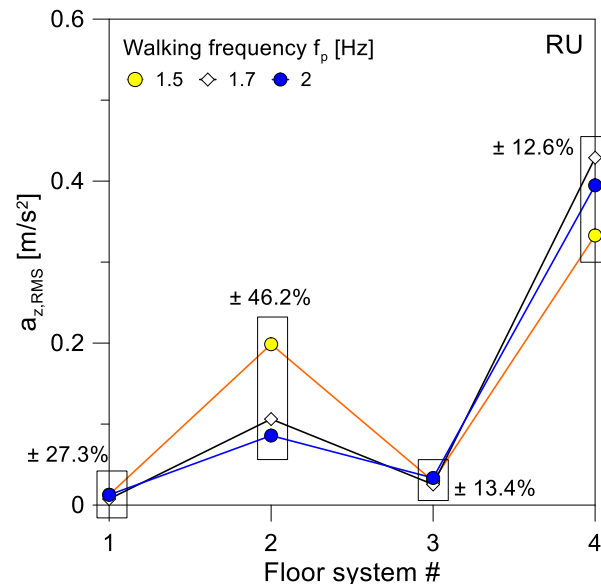
Figure 7. Numerical results for F#1 to F#4 floor systems, based on equivalent-force calculations (RU model), in terms of RMS acceleration, as a function of walking frequency f_p (ABAQUS).

Thus, the RMS value in Figure 7, for example, increases from F#1 to F#2 with the increase of flexibility of the concrete slabs. Indeed, the RMS estimates are counterintuitive for F#3 and F#4, where maximum peaks are found with the F#4 system, which has a relatively high vibration frequency compared to F#3. As an additional parameter of comparison, the mass ratio is particularly small, especially for F#4, compared to the other systems summarized in Table 1. Note in Figure 7 that comparing the F#1 and F#3 systems with similar mass ratio ($\approx 1/130$th) but different vibration frequency, f1 is still in line with expectations, where the RMS is higher for the flexible system F#3.

For the F#4 system with limited structural mass but still relatively high vibration frequency, on the other side, the RMS acceleration values due to the pedestrian is more than twice compared to F#3 system with lower vibration frequency but still high structural mass. Also, F#4 estimates are mostly twice the F#2 concrete system with low frequency. These preliminary observations for glazed floors are in line with previous research studies on glass applications for pedestrian systems (see for example [16–20]) and suggest the need for further research efforts for these structural typologies under ordinary design conditions.

4.2. High-Mass Floor Sensitivity to Loading Strategy

A second comparative analysis of parametric numerical results was focused on floor systems F#1 to F#3, in which the structural mass M_s is high compared to the occupant. Still, major variations can be noted in terms of vibration frequency (Table 1).

Results are collected in Figures 8 and 9 in terms of RMS value, acceleration peak or CREST factor trends for the examined walking frequencies. In addition, the numerical outcomes from the selected SMD models are also compared to the RU modelling approach.
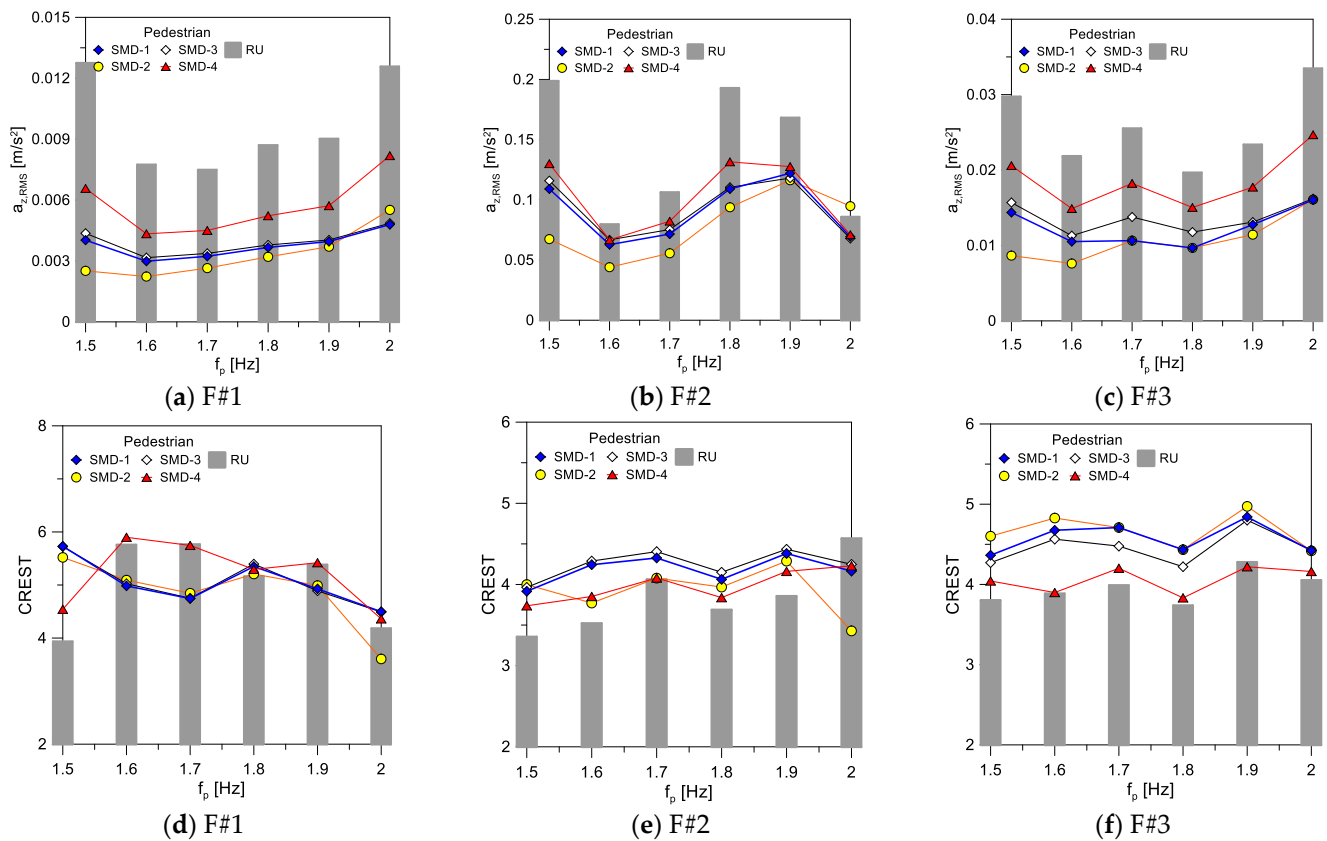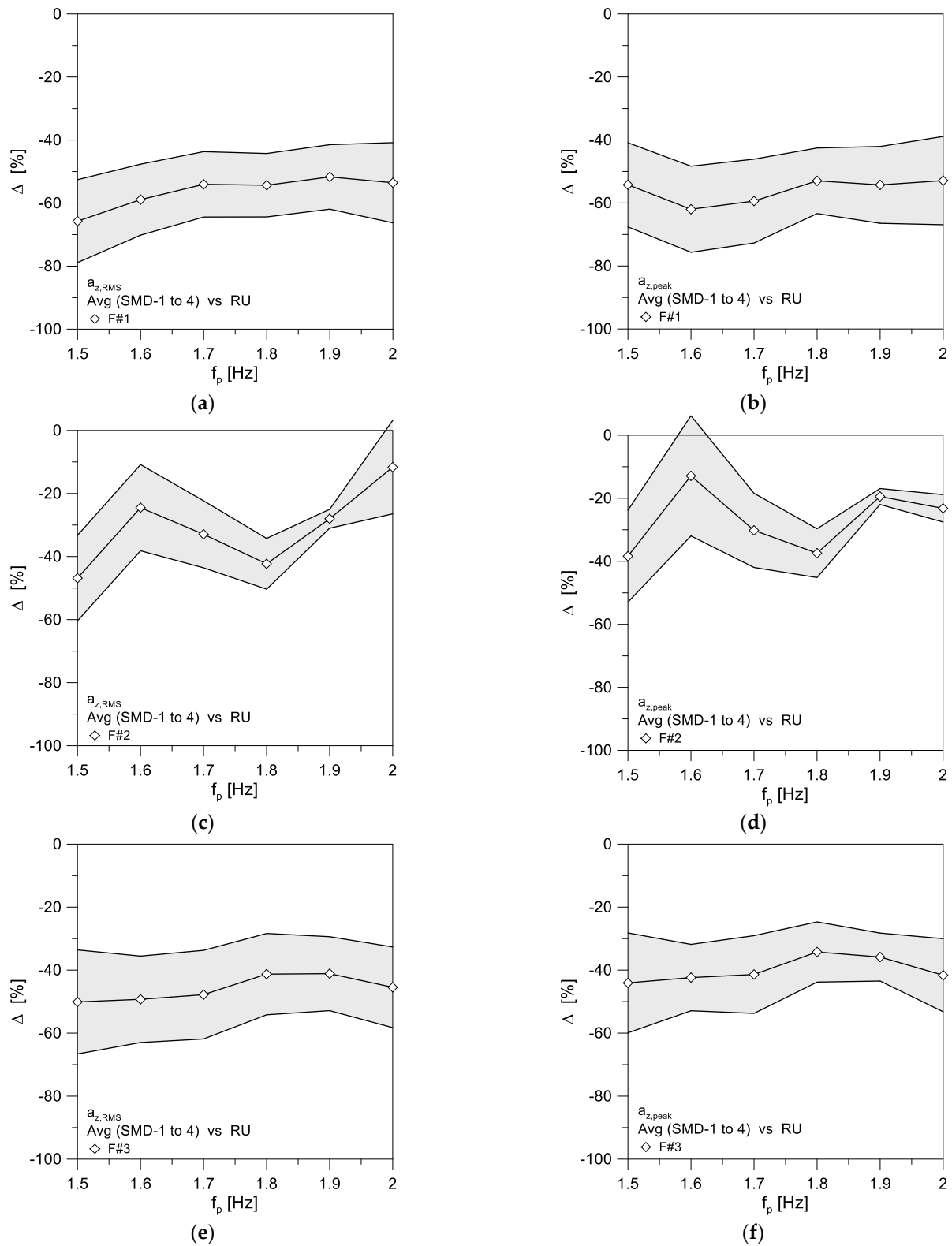
Figure 8. Numerical results for F#1, F#2 (concrete) and F#3 (glass) systems, based on different SMD or RU calculations, in terms of (**a**–**c**) RMS acceleration or (**d**–**f**) CREST factor, as a function of walking frequency f_p (ABAQUS).

Figure 8 shows that the performance indicators of floors F#1 to F#3 show a typically large scatter between the selected SMD models or the RU assumption. This suggests, in terms of vibration serviceability assessment and verification purposes (once experimental methods and records are not available in support of numerical tools), that the RU modelling strategy is generally more conservative than the examined SMD models. Under the lack of more specific comparative data or calculation methods, in this sense, the RU assumption should be preferred for a verification check. Still, it would necessitate, on the other side, an over-design of examined floor systems to satisfy conventional vibration limits.

In terms of different SMD formulations, for most of the proposed numerical pieces of evidence, it can be noted in Figure 8 that the SMD-4 approach has the minimum scatter towards RU, tending to overestimate the acceleration estimates of SMD-1-to-3 formulations and to underestimate the corresponding CREST. This effect can be noted for all F#1, F#2 and F#3 systems, regardless of the dynamic features of structural systems in terms of vibration frequency, and assuming a relatively "high" structural mass for them. Similarly, the SMD-2 model tends to underestimate the numerical predictions of the other formulations in terms of RMS acceleration and peak for all the examined configurations.

In terms of quantitative analysis of results, the major scatter was indeed noted in terms of RMS and peak accelerations, especially for F#1 and F#3 systems, which are characterized by low-medium vibration frequency f_1 and high, similar mass M_s, compared to the occupant. The corresponding percentage scatter of SMD averages to RU calculations is proposed in Figure 9 as a function of the imposed walking frequency. Note that for F#1 and F#3, the maximum scatter is estimated in the range of 30%. For the F#2 system only, the calculated percentage scatter is less pronounced in terms of absolute value, especially for faster walks ($f_p > 1.8$ Hz). Still, on the other side, it is more sensitive to the walking

frequency f_p, due to additional interaction with motion harmonics, with up to +40% of the variation for $f_p < 1.8$ Hz.

Figure 9. Numerical results for (**a**,**c**,**e**) RMS acceleration and (**b**,**d**,**f**) peak acceleration for F#1, F#2 and F#3 systems, in terms of SMD (average ± standard deviation) to RU percentage scatter, as a function of walking frequency f_p (ABAQUS).

4.3. Low-Mass Floor Sensitivity to Loading Strategy

When the selected SMD models are applied to the presently explored F#4 system, it is possible to expect a typical response like in Figure 10. In terms of RMS value, see Figure 10a, the trend of acceleration output with the walking frequency is mostly in line for all the SMD approaches, and the RMS acceleration increases with f_p. Furthermore, a very close correlation of numerical estimates can be noted, especially for SMD-1 and SMD-3 models (7.4% of their scatter in the range $f_p = 1.5 \div 2$ Hz).
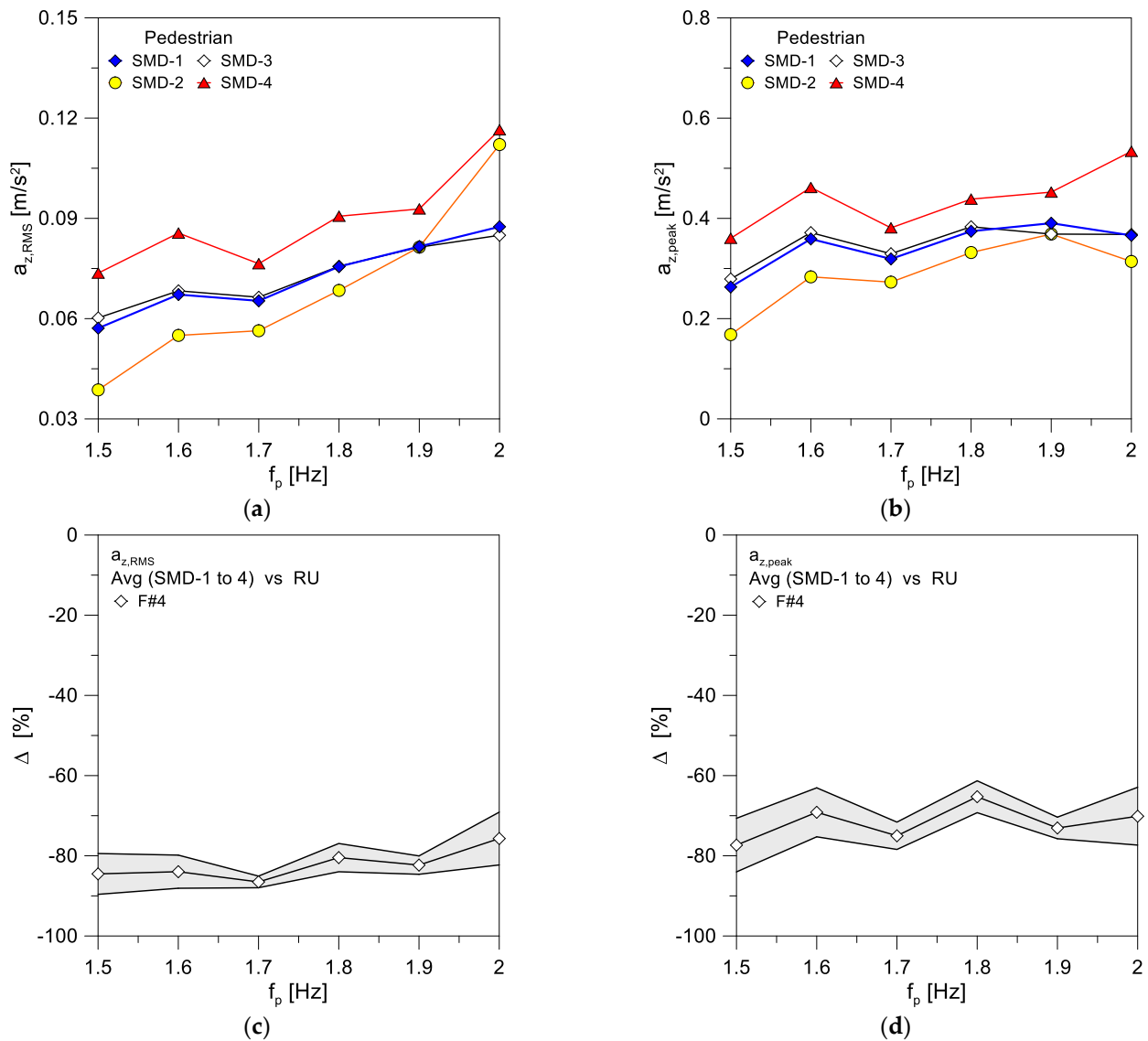
Figure 10. Numerical results for the glazed F#4 system, based on different SMD or equivalent-force calculations: (**a**) RMS acceleration and (**b**) peak acceleration, as a function of walking frequency f_p, with (**c**,**d**) corresponding SMD (average ± standard deviation) to RU percentage scatter (ABAQUS).

The SMD-4 formulation, see Figure 10a, generally tends to overestimate the effect of pedestrian (+43.5% compared to other SMD models for the examined f_p range), while the SMD-2 approach underestimates the other modelling strategies, especially for low walking frequencies f_p (−10.7% for the RMS acceleration). In terms of acceleration peak trend, as in Figure 10b, a similar dynamic response can be noted for the F#4 system. As a significant consequence, the corresponding CREST factor from Equation (20) also has marked sensitivity to different SMD models and input biodynamic parameters.

On the other side, it should be reminded from Table 1 that the F#4 slab has a relatively low mass but still high frequency. Figure 10c,d, in this regard, shows the corresponding average (±standard deviation) of SMD averages towards the RU model estimates in percentage scatter. Under RU assumption and high frequency, the SMD approach overestimates the RU predictions in the same order of magnitude of F#1 and F#3 floor systems. Conversely, the magnitude of percentage scatter is significantly reduced compared to Figure 9, less than 15%, thus suggesting a more stable trend of various SMD estimates with f_p.

4.4. Comparison of Low-Frequency and Low-Mass Floors

Regardless of the reference limit values for performance indicators to verify, the analysis of acceleration output on F#1 to F#4 systems for the examined walking configurations suggests, on one side, a large sensitivity to modelling assumptions, and on the other side a similar structural sensitivity for pedestrian systems with low-frequency and/or low-mass respectively.

Such an outcome can be noted, for example, in Figure 11, where RMS and peak accelerations from $f_p = 1.5 \div 2$ Hz interval are reported as a function of frequency ratio f_1/f_p. In this way, it is possible to see that the F#2 and F#4 systems described in Table 1 have comparable acceleration amplitudes, even characterized by markedly different structural parameters (mass and vibration frequency). Furthermore, for the F#1 and F#3 systems with similar mass ratios and vibration frequencies slightly above 8 Hz, the comparative results in Figure 11 have a qualitative and quantitative agreement. Most importantly, it is to note that the F#4 system, differing from F#2, has a high vibration frequency, which is mostly twice the reference threshold of 8 Hz which is recommended for vibration serviceability issues, but very small mass, compared to the occupant and to the other floor configurations.
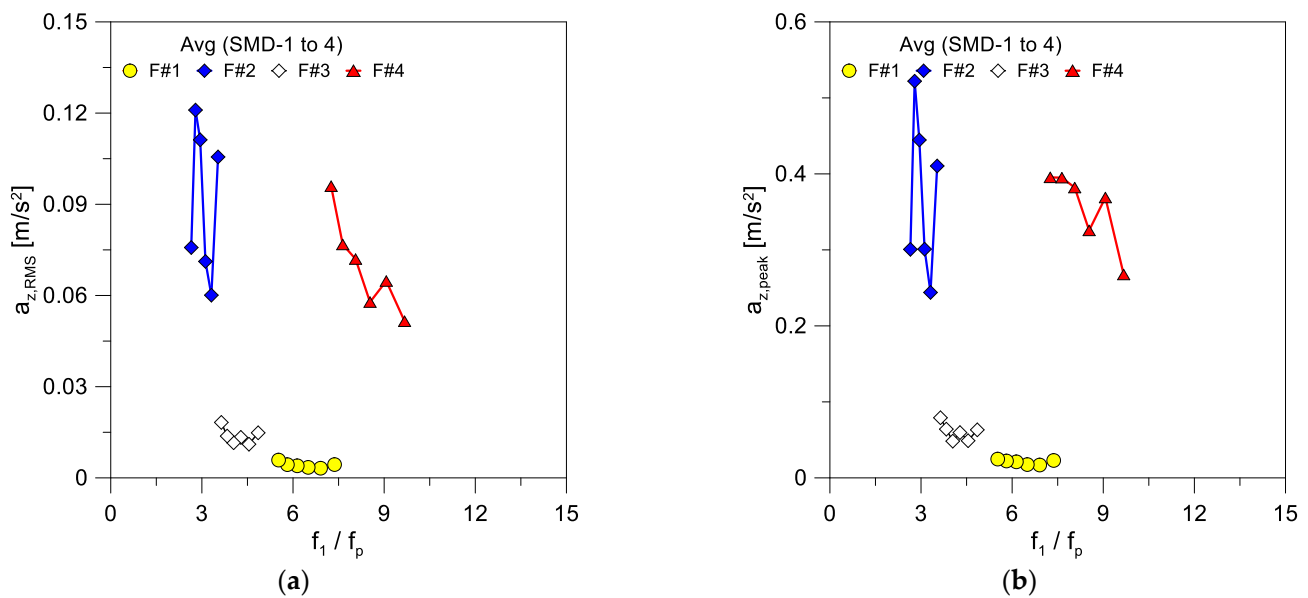
Figure 11. Numerical results for (**a**) RMS acceleration and (**b**) peak acceleration on F#1, F#2, F#3 and F#4 systems, in terms of SMD (average), as a function of vibration frequency f_1 to walking frequency f_p ratio (ABAQUS).

For the F#2 and F#4 floor systems, final attention can be spent on the analysis of SMD effects on basic performance indicators for vibration serviceability, namely RMS value and peak of technical interest towards conventional limits for verification. Both these systems are taken into account because the first one, F#2, is a typical slender slab with very small frequency and high mass, while F#4 is representative of a "new" glazed solution.

Figure 12a,b shows the average RMS value as a function of walking frequency under various SMD assumptions and the scatter of standard deviation. It can be noted that the scatter is rather uniform with f_p variations. Also, as previously discussed, the F#2 system is largely sensitive to fp, whilst this effect is less pronounced for the stiffer F#4 system. Most importantly, the comparisons in Figure 12c in terms of standard deviation and percentage scatter from the average of SMD estimates of the selected models give evidence of a rather good agreement for both F#2 and F#4 systems, thus confirming that both low-frequency and low-mass structural solutions should be verified with dedicated tools.
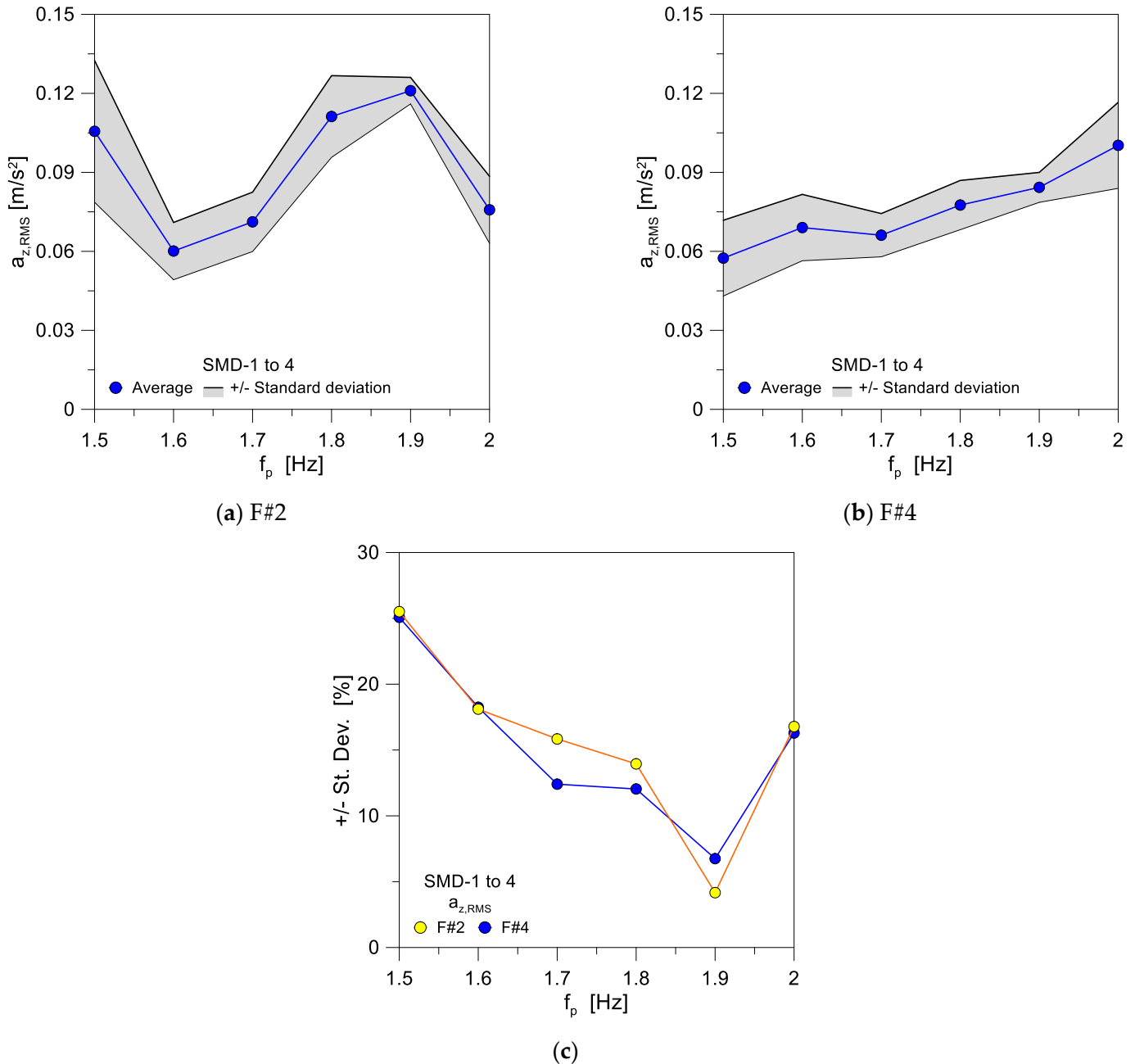
Figure 12. Sensitivity of RMS acceleration to selected SMD pedestrian models (with *M* = 80 kg) for floor systems: (**a**) F#2 (concrete) and (**b**) F#4 (glass) configurations, with (**c**) trend of percentage scatter for both systems (ABAQUS).

5. Conclusions

For structural vibration issues, knowledge and availability of computationally efficient and realistic modelling strategies represent a strategic task. Over the years, several formulations and proposals have been theoretically elaborated in the literature and validated towards experimental investigations. These efforts supported a more realistic analysis of vibration issues and Human-Structure Interaction (HSI) phenomena, especially for low-frequency structural systems (like bridges and walkways) characterized by high sensitivity to vibrations.

In this paper, among others, the attention was focused on a literature selection of Spring-Mass-Damper (SMD), Single Degree of Freedom (SDOF) approaches to describe the vertical loads induced by a single pedestrian on a given structural system (SMD-1 to SMD-4), in terms of calibrated equivalent mass m, spring stiffness k and damping coefficient c. The parametric numerical analysis (inclusive of 100 different configurations) was focused on four different floors (F#1 to F#4) with various combinations of vibration frequency f_1 and structural mass M_s, compared to the walking pedestrian (with mass M and moving at f_p). From the selected SMD models, it was shown, for example, that calibrated (m, k, c) parameters may strongly differ from each other, even to describe the same walking pedestrian/walking setup. Accordingly, modifications can also be expected in terms of predicted structural behaviours and performance indicators of the examined floors (like acceleration peak, RMS acceleration, CREST factor, etc.), which are of significant interest for vibration serviceability assessment. Furthermore, such sensitivity can be further affected by the intrinsic dynamic parameters of those floor systems most sensitive to human-induced loads.

Through the parametric numerical analysis carried out in ABAQUS, the attention was thus focused on two concrete floors with medium or low vibration frequency but relatively high structural mass compared to the occupant (F#1 and F#2, with mass ratio > 1/40th). The third and fourth systems (F#3 and F#4) were made of glass and characterized by low or medium vibration frequency but still high or rather small mass respectively, compared to the pedestrian ($\approx$1/4th the mass ratio for F#4 system).

The parametric study proved that SMD models are more stable and less scattered in dynamic estimates on the structural side as far as they are applied to low-frequency systems with high mass. Besides, for low-mass systems, such as modular slabs composed of glass, which are characterized by specific intrinsic features compared to traditional structural solutions, the numerical predictions emphasized a relatively high scatter of reference performance indicators based on various SMD models of literature. Also, the SMD-based sensitivity of structural parameters under the effects of the same pedestrian was measured at up to 30% from the average for F#2 and F#4 systems, thus denoting a primary role of low-frequency for floor sensitivity, but also low-mass, as a critical additional influencing parameter, regardless the vibration frequency. As such, additional investigations and dedicated calibrations are needed for this special typology of pedestrian systems.

References

1. Bachmann, H.; Ammann, W. *Vibrations in Structures: Induced by Man and Machines*; International Association for Bridge and Structural Engineering: Zurich, Switzerland, 1987.
2. Sedlacek, G.; Heinemeyer, C.; Butz, C. *Generalisation of Criteria for Floor Vibrations for Industrial, Office, Residential and Public Building and Gymnasium Halls*; European Commission: Luxembourg, 2006.
3. Shahabpoor, E.; Pavic, A.; Racic, V. Interaction between Walking Humans and Structures in Vertical Direction: A Literature Review. *Shock Vib.* **2016**, *2016*, 3430285. [CrossRef]
4. Zhang, M.; Georgakis, C.T.; Chen, J. Biomechanically excited SMD model of a walking pedestrian. *J. Bridge Eng.* **2016**, *21*, C4016003. [CrossRef]
5. Silva, F.T.; Brito, H.M.B.F.; Pimentel, R.L. Modelling of crowd load in vertical direction using biodynamic model for pedestrians crossing footbridges. *Can. J. Civ. Eng.* **2013**, *40*, 1196–1204. [CrossRef]
6. Toso, M.A.; Gomes, H.M.; da Silva, F.T.; Pimentel, R.L. Experimentally fitted biodynamic models for pedestrian-structure interaction in walking situations. *Mech. Syst. Signal Process.* **2016**, *72–73*, 590–606. [CrossRef]
7. Pfeil, M.S.; Varela, W.D.; de Paula Amador da Costa, N. Experimental calibration of a one degree of freedom biodynamic model to simulate human walking-structure interaction. *Eng. Struct.* **2022**, *262*, 114330.
8. Wang, H.; Chen, J.; Brownjohn, J.M.W. Parameter identification of pedestrian's spring-mass-damper model by ground reaction force records through a particle filter approach. *J. Sound Vib.* **2017**, *411*, 409–421. [CrossRef]
9. Pena, A.N.P.; de Brito, J.L.V.; da Silva, F.F.G.; Pimentel, R.L. Pedestrian Biodynamic Model for Vibration Serviceability of Footbridges in Lateral Direction. *J. Vib. Eng. Technol.* **2021**, *9*, 1223–1237. [CrossRef]
10. Bocian, M.; Macdonald, J.H.G.; Burn, J.F. Biomechanically inspired modeling of pedestrian-induced vertical self-excited forces. *J. Bridge Eng.* **2013**, *18*, 1336–1346. [CrossRef]
11. Koopman, B.; Grootenboer, H.J.; de Jongh, H.J. An inverse dynamics model for the analysis, reconstruction and prediction of bipedal walking. *J. Biomech.* **1995**, *28*, 1369–1376. [CrossRef] [PubMed]
12. Geyer, H.; Seyfarth, A.; Blickhan, R. Compliant leg behaviour explains basic dynamics of walking and running. *Proc. R. Soc. Biol. Sci.* **2006**, *273*, 2861–2867. [CrossRef] [PubMed]
13. Yang, Q.S.; Qin, J.W.; Law, S.S. A three-dimensional human walking model. *J. Sound Vib.* **2015**, *357*, 437–456. [CrossRef]
14. *CEN/TC 250*; prCEN/TS xxxx-1, 2019—In-Plane Loaded Glass Components. CEN—European Committee for Standardization: Brussels, Belgium, 2019.
15. *CEN/TC 250*; prCEN/TS xxxx-2, 2019—Out of-Plane Loaded Glass Components. CEN—European Committee for Standardization: Brussels, Belgium, 2019.
16. Bedon, C. Experimental investigation on vibration sensitivity of an indoor glass footbridge to walking conditions. *J. Build. Eng.* **2020**, *29*, 101195. [CrossRef]
17. Bedon, C. Diagnostic analysis and dynamic identification of a glass suspension footbridge via on-site vibration experiments and FE numerical modelling. *Compos. Struct.* **2019**, *216*, 366–378. [CrossRef]
18. Bedon, C.; Noè, S. Post-Breakage Vibration Frequency Analysis of In-Service Pedestrian Laminated Glass Modular Units. *Vibration* **2021**, *4*, 836–852. [CrossRef]
19. Bedon, C.; Noè, S. Uncoupled Wi-Fi Body CoM Acceleration for the Analysis of Lightweight Glass Slabs under Random Walks. *J. Sens. Actuator Netw.* **2022**, *11*, 10. [CrossRef]
20. Bedon, C.; Fasan, M.; Noè, S. Body Motion Sensor Analysis of Human-Induced Dynamic Load Factor (DLF) for Normal Walks on Slender Transparent Floors. *J. Sens. Actuator Netw.* **2022**, *11*, 81. [CrossRef]
21. *ABAQUS Computer Software v.6.14*; Simulia: Dassault, RI, USA, 2021.
22. Varela, W.D.; Pfeil, M.S.; da Costa, N.P.A. Experimental investigation on human walking loading parameters and biodynamic model. *J. Vib. Eng. Technol.* **2020**, *8*, 883–892. [CrossRef]
23. Clough, R.W.; Penzien, J. *Dynamics of Structures*; McGrawHill: Berkeley, CA, USA, 1993.